Dynamic surface-enhanced Raman spectroscopy of DNA oligomer with a single hotspot from a gold nanoparticle dimer

Sugano, Koji
Maruoka, Katsunari
Ikegami, Kohei
Uesugi, Akio
Isono, Yoshitada

(Citation)
Optics Letters,47(2):373-376

(Issue Date)
2022-01-15

(Resource Type)
journal article

(Version)
Accepted Manuscript

Dynamic surface-enhanced Raman spectroscopy of DNA oligomer with a single hotspot of a gold nanoparticle dimer

KOJI SUGANO,* KATSUNARI MARUOKA, KOHEI IKEGAMI, AKIO UESUGI, YOSHITADA ISONO

Department of Mechanical Engineering, Graduate School of Engineering, Kobe University, Kobe, 657-8501, JAPAN
**Corresponding author: sugano@mech.kobe-u.ac.jp*

Received XX Month XXXX; revised XX Month, XXXX; accepted XX Month XXXX; posted XX Month XXXX (Doc. ID XXXXX); published XX Month XXXX

Various nanostructures for single-molecule surface-enhanced Raman spectroscopy (SERS) have been fabricated through a random aggregation process using nanoaprticles that can stochastically generate multiple hotspots in the laser spot. This leads to the multiple molecule detection. In this study, a single gold nanoparticle (AuNP) dimer with a single hotspot was fabricated in a laser spot controlling the position and orientation on a silicon substrate using a nanotrench-guided self-assembly. The Raman peaks of the DNA were dynamically observed, indicating a single DNA oligomer detection composed of adenine, guanine, cytosine, phosphate, and deoxyribose.

Surface-enhanced Raman spectroscopy (SERS) is a direct, label-free, and highly sensitive analytical tool used in the detection and analysis of biomolecules, such as macromolecular proteins and DNA nucleobases, through their intrinsic Raman fingerprint [1-3]. In addition, this spectral technique is highly dependent on the physiochemical properties of the substrate materials, such as nanoscale plasmonic structures (e.g., gold) that realize electromagnetic localization and enhancement (i.e., weak Raman signals can be significantly enhanced). In general, SERS allows for single-molecule detection and identification, making it possible to carry out label-free DNA analysis such as DNA sequencing with excellent molecule identification capacity.

Next-generation sequencing of DNA using fluorescent probes requires polymerase chain reaction (PCR) to amplify the fragmented DNA, obtaining a sufficient number of DNA fragments for detectable signal and DNA sequence reconstruction. However, using PCR is expensive, time-consuming, and necessitates further fragmentation, resulting in the occurrence of a sequencing error due to shorter fragments. On the other hand, several previous studies have reported on the electrical detection and identification of DNA using nanopore [4] or nanoelectrode [5, 6], which do not require for the amplification and labeling of the fluorescent probes. This direct analytical method is a powerful tool for high-speed and low-cost processes. However, one of the major drawbacks of this method is the large variation of the electrical signal, leading to a low reliability of the DNA sequencing. To address this limitation, employing a single-molecule SERS is advantageous due to its higher identification capability compared to electrical methods because the SERS spectrum includes several Raman peaks derived from DNA components. Random DNA sequencing is expected by measuring continuous Raman peak transitions from time-series Raman spectra of a single DNA oligomer. Dynamic measurements of a single DNA oligomer with a single plasmonic hotspot is required for SERS-based DNA sequencing.

Several SERS studies have been conducted on DNA oligomer detection and identification using particle aggregates [1, 2, 7]. Specifically, the random aggregation of nanoparticles generates nanogaps with highly enhanced hotspots. A nanoparticle dimer or a straight nanoparticle chain is considered as a nanostructure with the highest Raman enhancement at the narrow nanogap between nanoparticles [8-11]. It results in a stochastic detection of a single molecule while matching the polarization direction of the incident laser and the connecting direction of the nanoparticles on a substrate [12, 13]. However, the nanostructures used in these studies could randomly generate multiple hotspots in the laser spot, because of uncontrollable positioning of particles, leading to the Raman measurement of multiple molecules. On the one hand, dynamic measurements of a single DNA oligomer by using nanoparticle aggregates or a nanoparticle dimer has not yet been reported. On the other hand, Chen et al. [14] reported about the dynamic SERS measurement of a single DNA oligomer through a gold nanoslit. The nanoslit stochastically forms nanogaps with a sensitivity for a single DNA oligomer detection. The stochastic fabrication process is considered to lead to the low probability of the single molecule detection and the detection of the multiple DNA oligomers with multiple hotspots.

In this study, we propose a nanotrench-guided self-assembly [15, 16] to fabricate only a single gold nanoparticle (AuNP) dimer, controlling its position and orientation on a substrate; this allows for a single hotspot and higher probability of enhancement factor

for the single molecule sensitivity than those in the nanoslit, in the area of the laser spot. Because the previously reported AuNP dimers were randomly and stochastically generated, controlling the number of the AuNP dimers was difficult, resulting in multiple hotspots on the laser spot. In addition, the connecting direction of the AuNPs was uncontrollable, and thus the polarization direction of the incident laser must be adjusted for a single-molecule detection sensitivity. A single AuNP dimer was fabricated on the laser spot to ensure molecule detection at a single hotspot. We performed dynamic SERS measurements using the fabricated single AuNP dimer to confirm the possibility of single-DNA oligomer detection as a challenging application such as in SERS-based DNA sequencing.

The AuNP dimer is composed of two AuNPs that form a nanogap between them. The AuNP dimers were fabricated on the Si substrate using the top-down and bottom-up processes. First, we fabricated nanoscale trenches on the Si substrate using electron-beam lithography and subsequent reactive ion dry etching of Si using SF_6 gas. Rectangular trenches were used as a template to form the AuNP dimer by a self-assembly bottom-up process. The width, length, and depth of the nanotrench were 86, 214, and 45 nm, respectively. AuNP colloids with a mean diameter of 100 nm were used, which were dispersed in a water suspension. The nanotrench on the Si substrate traps the AuNPs while the AuNP colloidal solution dries on the Si substrate because the water suspension pushes the AuNPs to the substrate surface by interfacial force. After the water suspension passed through the nanotrench, two AuNPs were held on the nanotrench and then made contact with each other by the water bridge force. AuNPs were modified with molecules such as citrate, acetonedicarboxylic acid, and acetoacetic acid when they are chemically synthesized by a citrate-reduction method [17, 18]. The molecules on AuNP surfaces were removed by ultraviolet ozone (UV/O_3) treatment to form nanogaps, which can be used as hotspots for enhancing the Raman scattering light, between AuNPs. The nanogap was estimated to be approximately 1 nm because the molecules on AuNP surfaces have been reported to be 0.5 nm in length [19]. The AuNPs were arranged along the nanotrench, and the nanotrench pattern determined the AuNP connecting direction. We can easily match the polarization direction of the incident laser to the connecting direction of the AuNPs.

The AuNP dimers were arrayed on the substrate with an interval of 5 μm to ensure that the laser light illuminated only a single AuNP dimer in the laser spot with a diameter of 2 μm. The AuNP dimers were fabricated at the designated position and arrayed on a substrate with a designated interval. This means that a hotspot, which acts as a molecular measurement point, is placed at a designated position, and a single hotspot is guaranteed for single-molecule SERS measurements. Figure 1(a)–(c) show the images of the fabricated AuNP dimer using scanning electron microscopy (SEM) and transmission electron microscopy (TEM). We observed only a single AuNP dimer in the laser spot.

The electromagnetic enhancement factor of the AuNP dimer was calculated using the finite differential time domain (FDTD) simulation. The simulation model included the AuNP dimer on the Si substrate with a 1-nm nanogap. The polarization direction was set parallel to the direction of the AuNP connection. Figure 1(d) shows the contour plot of the electromagnetic enhancement factor $|E_l|^2$ at a laser wavelength of 632.8 nm, indicating the enhanced electromagnetic field at the nanogap with a maximum $|E_l|^2$ of 7.8×10^5.

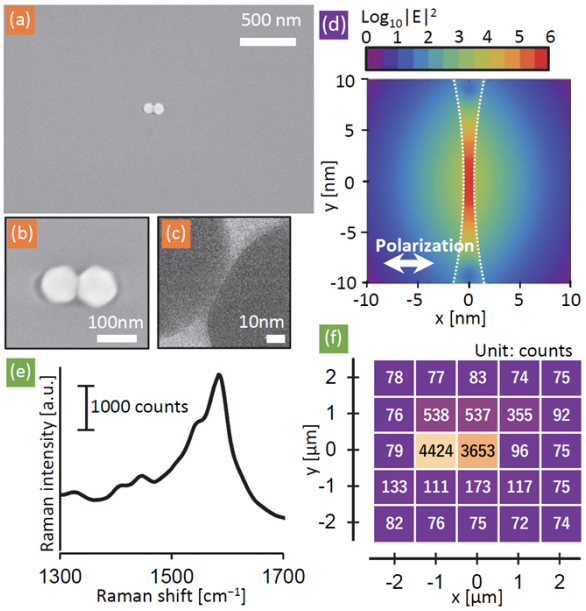

Fig. 1. AuNP dimer with a mean diameter of 100 nm on the Si substrate. (a), (b) SEM image of isolated AuNP dimer, (c) TEM image of nanogap. (d) Contour plot of the electromagnetic enhancement factor at nanogap calculated through FDTD simulation. (e), (f) Raman spectrum and contour plot of Raman intensity in mapping measurement around the AuNP dimer before removing the attached molecule on AuNP surfaces. The unit of the Raman intensity is counts.

The measurements were performed using a Raman spectroscopy apparatus with a 632.8-nm He–Ne laser used for excitation with a laser spot of 2 μm, a laser intensity of 8.2 mW, and a 50× objective lens (N.A. 0.5). The SERS study on DNA oligomers detection used 8 mW laser irradiation and reported no damage to DNA oligomer in Ref. [14]. The laser irradiation with 8.2 mW used in this study is thought to give no damage to DNA oligomers. The piezoactuator stage equipped in the microscope allowed for the alignment of the laser spot. Moreover, we determined the optimal position for the highest Raman intensity after performing the mapping measurements around the AuNP dimer. The arrayed AuNP dimers point in a uniform direction and allow for effective measurements by scanning the laser spot without matching the polarization angle. Figures 1(e) and (f) show the experimental Raman spectrum and Raman intensity distribution acquired from mapping the Raman measurements before removing the attached molecules on the AuNP surfaces, which involved citrate, acetonedicarboxylic acid, and acetoacetic acid. The unit of the Raman intensity is counts. The Raman spectrum shows a strong Raman intensity from the attached molecules at Raman shifts ranging from 1500 to 1700 cm^{-1}, as shown in Fig. 1(e). We evaluated the Raman enhancement and its distribution by mapping Raman measurement with an integration time of 1 s and a mapping interval of 1 μm. This experiment was performed because the Raman intensity before UV/O_3 treatment reflects the Raman intensity of the target DNA molecule after UV/O_3 treatment [13]. Figure 1(f) shows the maximum Raman intensity in the Raman shift range from 1500 to 1700 cm^{-1}. We observed locally enhanced points with the largest Raman intensity. The laser spot diameter and mapping interval were 2 and 1 μm, respectively. We confirmed a single enhancing site that corresponds to the position of the AuNP dimer and determined the measurement point using the obtained mapping results.

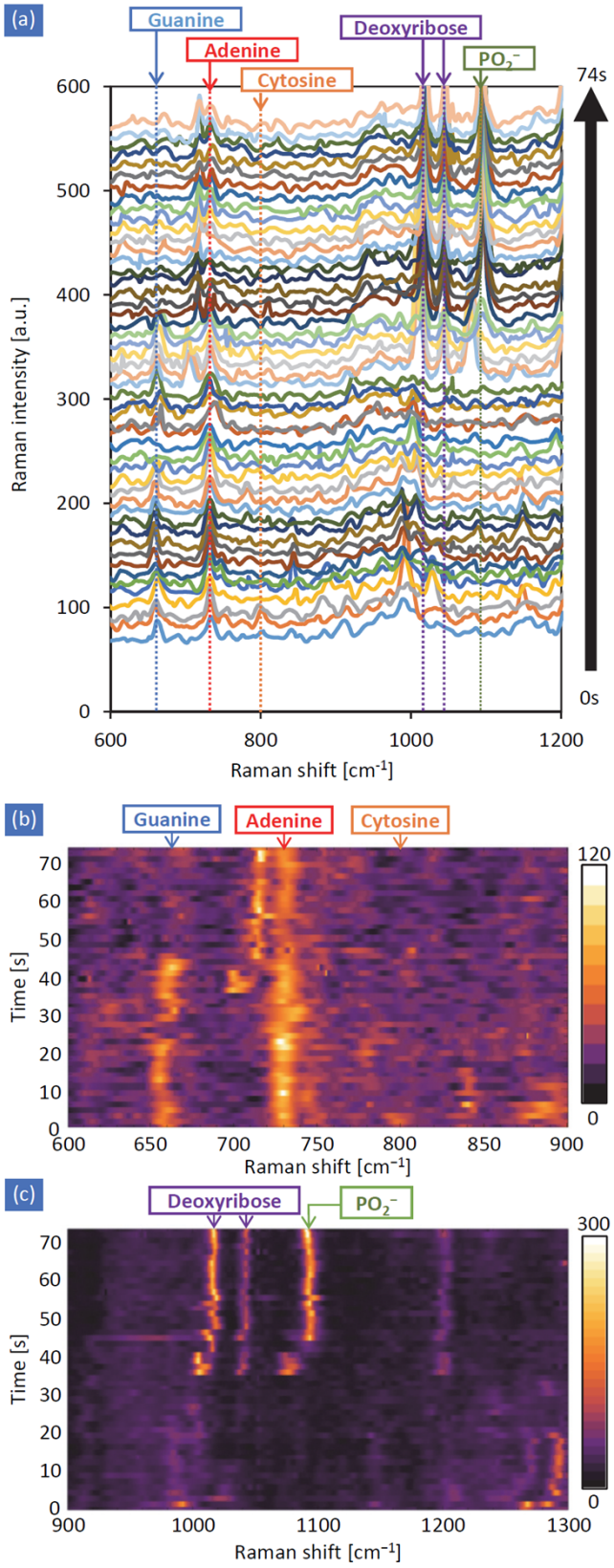

Fig. 2. Fifty generated Raman spectra from the DNA oligomer solution using a single AuNP dimer. Intermitted Raman spectroscopy measurement was carried out with an integration time of 0.5 s and an interval of 1.0 s. (a) Stacked Raman spectra. Contour plots of the Raman spectra as a function of the elapsed time at the Raman shift with a range of (b) 600–900 and (c) 900–1300 cm^{-1}.

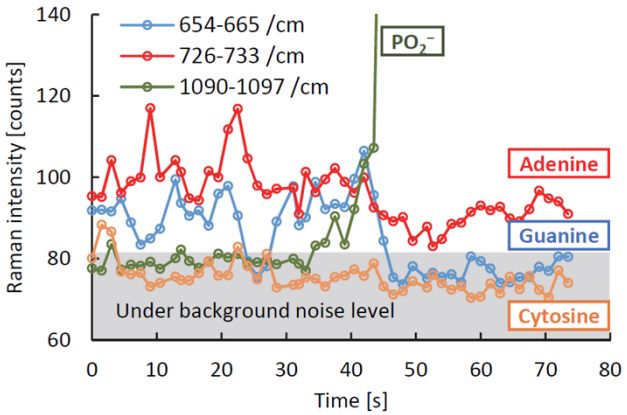

Fig. 3. Transition of Raman intensities in four Raman shift bands that indicates guanine, adenine, cytosine, and PO^{2-}. The gray area indicates the background noise level. Raman intensity of PO^{2-} increased more than 170 counts after 45 s.

DNA samples were purchased from Fasmac Co., Ltd. (Japan). The sequence of the single-stranded DNA measured in this experiment was 5'-AGCTAGCT-3'. The DNA concentration was 100 μM in the TE buffer solution, which was placed in polydimethylsiloxane (PDMS) well. We acquired the Raman spectra at an integration time of 0.5 s by intermittent Raman measurements with an interval of 1.0 s. The total measurement time was 74 s to acquire the time-series of 50 Raman spectra.

Figure 2(a) shows 50 Raman spectra obtained from 0 to 74 s. The contour plots of the Raman spectra created based on Fig. 2(a) are shown in Fig. 2(b) and (c), wherein the two plotting graphs are separated with different ranges of the Raman shifts. We confirmed that several Raman peaks derived from the DNA were observed from the single AuNP dimer with a measurement time of 0.5 s based on the acquired Raman spectra as shown in Fig. 2(a)-(c). We observed the Raman peaks of phosphate (PO^{2-}) at 1093 cm^{-1} and deoxyribose at 1017 and 1043 cm^{-1}, indicating the C-O stretching mode, as the DNA backbone [20, 21]. Furthermore, we observed the Raman peaks of adenine, guanine, and cytosine at around 730, 660, and 799 cm^{-1}, respectively, as the DNA base [22]. The detection of the DNA compositions indicates that the single AuNP dimer can be used for single DNA oligomer detection because of the limited space of the single hotspot with a nanogap between AuNPs of approximately 1 nm.

We observed the transition of the acquired Raman spectra, as shown in Figs. 2 and 3, in all 50 Raman measurements. Figure 3 shows the time series of the Raman intensities of the selected Raman shift bands, indicating guanine, adenine, cytosine, and deoxyribose. Guanine was first detected from 0 to 22.5 s, disappeared from 24 to 27 s, and reappeared at 28.5 to 40 s. On the other hand, the Raman peak of cytosine was observed only at the beginning of the measurements. Meanwhile, the Raman peaks of adenine were observed in all spectra. The adenine band was clearly observed at approximately 730 cm^{-1}, as shown in Fig. 2(b). Both the backbone peaks from PO^{2-} and deoxyribose suddenly appeared at approximately 42 s at the same time, which is related to the disappearance of the guanine peak, and maintained high intensity until the end of the measurements. Moreover, coupled transitions of the guanine and backbone Raman signals were observed. The disappearance and appearance of guanine, cytosine, and backbone signals support the possibility of single DNA detection and dynamic measurement of a moving DNA.

We considered that the proposed AuNP dimer detects a single DNA oligomer based on the Raman signal transition and limited space of the hotspot. Particularly, the Raman scattering cross-section of adenine was reported to be 2.9×10^{-30} cm^2/sr, and an enhancement factor of 7.1×10^{10} is necessary for the single-molecule detection of adenine [23]. The maximum Raman enhancement factor for the adenine peak at 730 cm^{-1} was calculated to be 3.0×10^{11} using $|E_I|^2\times|E_R|^2$ [24]. Here, $|E_I|^2$ and $|E_R|^2$ are the electromagnetic enhancement factors at the wavelengths of the excitation laser light and Raman scattering light of adenine (663.7 nm corresponding to 730 cm^{-1}), respectively. Therefore, the Raman enhancement factor needs to be sufficiently large to detect a single adenine nucleobase.

Results show that adenine was highly detectable compared to other nucleobases, owing to its binding affinity to Au surfaces and higher Raman scattering cross-section [1, 7, 25-27]. The binding of the molecule to the Au surface becomes easier with the increasing affinity, causing a higher Raman enhancement because the highest Raman enhancement is generated at surfaces of the narrowest nanogap. The Raman peak at 730 cm^{-1} is apparent owing to the binding of adenine to the Au surface, indicating that the oligomer is pinned with adenine binding on the Au surface that made adenine readily detectable. The other parts of the oligomer, except the attached adenine, are considered fluctuating in the vicinity of the Au surface while the adenine was trapped. Initially, guanine, cytosine, and backbone were thought to be detected, while they stochastically reached the enhancing hotspot with the necessary enhancement factor to be detected. Results show that their peaks appeared and disappeared because of lower affinities than that of adenine [1, 25, 26], indicating the short duration of molecule binding on Au surfaces. On the other hand, thymine detection was difficult because its binding affinity to Au surfaces was the lowest among the four nucleobases [1, 28].

In conclusion, dynamic SERS measurements were performed to detect and identify single DNA oligomers and confirm the possibility of a single DNA oligomer detection using the isolated single AuNP dimer, which was fabricated on the Si substrate using the nanotrench-guided self-assembly, for single-hotspot detection in a laser spot. The nanotrench-guided self-assembly was able to control the position and connecting direction of the AuNP dimers. Results show that several Raman peaks derived from the DNA were observed from the single AuNP dimer with a measurement time of 0.5 s. We observed the Raman peaks of adenine, guanine, and cytosine, and the peaks of PO^{2-} and deoxyribose as the DNA backbone. Moreover, the transition of the acquired Raman spectra is apparent in all 50 measurements. The Raman peaks of adenine were observed in all spectra, while the peaks of guanine, cytosine, and backbone signals were observed to appear and disappear. The dynamic detection of the DNA compositions indicates that the single AuNP dimer has the capability to perform a single DNA oligomer detection, owing to the transition of the Raman signal and the limited space of a single hotspot with an approximately 1-nm nanogap between AuNPs. Finally, the results of this study support the possibility of performing a dynamic measurement of a moving DNA, and will lead to SERS-based analysis of DNA sequences with a single nucleobase sensitivity through the manipulation of a DNA oligomer.

Funding. KAKENHI Grant Number 18H01847 and 19H02571, Japan Society for the Promotion of Science (501100001691)

Acknowledgments. This study was supported by the Kyoto Integrated Science and Technology Bio-Analysis Center for Raman spectroscopy and the Nano Technology Hub of Kyoto University in the "Nanotechnology Platform Project" for nanofabrication.

Disclosures. The authors declare no conflicts of interest.

Data availability. Data underlying the results presented in this paper are not publicly available at this time but may be obtained from the authors upon reasonable request.

References

1. E. Papadopoulou and S. E. Bell, Chemistry (Easton) **18**, 5394-5400 (2012).
2. K. Kneipp, H. Kneipp, V. B. Kartha, R. Manoharan, G. Deinum, I. Itzkan, R. R. Dasari, and M. S. Feld, Phys. Rev. E **57**, R6281 (1998).
3. K. Kneipp, Y. Wang, H. Kneipp, L. T. Perelman, I. Itzkan, R. R. Dasari, and M. S. Feld, Phys. Rev. Lett. **78**, 1667 (1997).
4. E. A. Manrao, I. M. Derrington, A. H. Laszlo, K. W. Langford, M. K. Hopper, N. Gillgren, M. Pavlenok, M. Niederweis, and J. H. Gundlach, Nat. Biotechnol. **30**, 349-353 (2012).
5. T. Ohshiro, Y. Komoto, M. Konno, J. Koseki, A. Asai, H. Ishii, and M. Taniguchi, Sci. Rep. **9**, 3886 (2019).
6. A. Morita, T. Sumitomo, A. Uesugi, K. Sugano, and Y. Isono, Nano Express **2**, 010032 (2021).
7. A. Barhoumi, D. Zhang, F. Tam, and N. J. Halas, J. Am. Chem. Soc. **130**, 5523-5529 (2008).
8. S. Nie and S. R. Emory, Science **275**, 1102-1106 (1997).
9. W. Li, P. H. Camargo, X. Lu, and Y. Xia, Nano Lett. **9**, 485-490 (2008).
10. V. V. Thacker, L. O. Herrmann, D. O. Sigle, T. Zhang, T. Liedl, J. J. Baumberg, and U. F. Keyser, Nat. Commun. **5**, 3448 (2014).
11. S. Kogikoski, K. Tapio, R. E. von Zander, P. Saalfrank, and I. Bald, Molecules **26**(2021).
12. K. Sugano, K. Aiba, K. Ikegami, and Y. Isono, Jpn. J. Appl. Phys. **56**, 06GK01 (2017).
13. K. Sugano, K. Ikegami, and Y. Isono, Jpn. J. Appl. Phys. **56**, 06GK03 (2017).
14. C. Chen, Y. Li, S. Kerman, P. Neutens, K. Willems, S. Cornelissen, L. Lagae, T. Stakenborg, and P. Van Dorpe, Nat. Commun. **9**, 1733 (2018).
15. T. Ozaki, K. Sugano, T. Tsuchiya, and O. Tabata, J. Microelectromechanical Syst. **16**, 746-752 (2007).
16. K. Sugano, T. Ozaki, T. Tsuchiya, and O. Tabata, Sens. Mater. **23**, 263-275 (2011).
17. C. Munro, W. Smith, M. Garner, J. Clarkson, and P. White, Langmuir **11**, 3712-3720 (1995).
18. K. Sugano, Y. Uchida, O. Ichihashi, H. Yamada, T. Tsuchiya, and O. Tabata, Microfluid. Nanofluid. **9**, 1165-1174 (2010).
19. M. Giersig and P. Mulvaney, Langmuir **9**, 3408-3413 (1993).
20. W. Ke, D. Yu, and J. Wu, Spectrochim. Acta A **55**, 1081-1090 (1999).
21. X. Yiming, Z. Zhixiang, Y. Hongying, X. Yan, and Z. Zhiyi, J. Photochem. Photobiol. B **52**, 30-34 (1999).
22. C. Otto, T. Van den Tweel, F. De Mul, and J. Greve, J. Raman Spectrosc. **17**, 289-298 (1986).
23. E. J. Blackie, E. C. L. Ru, and P. G. Etchegoin, J. Am. Chem. Soc. **131**, 14466-14472 (2009).
24. Y. Nishijima, Y. Hashimoto, L. Rosa, J. B. Khurgin, and S. Juodkazis, Advanced Optical Materials **2**, 382-388 (2014).
25. J. A. Huang, M. Z. Mousavi, Y. Zhao, A. Hubarevich, F. Omeis, G. Giovannini, M. Schutte, D. Garoli, and F. De Angelis, Nat. Commun. **10**, 5321 (2019).
26. K. M. Koo, A. A. I. Sina, L. G. Carrascosa, M. J. A. Shiddiky, and M. Trau, Anal. Methods **7**, 7042-7054 (2015).
27. K. F. Domke, D. Zhang, and B. Pettinger, J. Am. Chem. Soc. **129**, 6708-6709 (2007).
28. J. J. Storhoff, R. Elghanian, C. A. Mirkin, and R. L. Letsinger, Langmuir **18**, 6666-6670 (2002).

Full reference list

1. E. Papadopoulou and S. E. Bell, "Label-free detection of nanomolar unmodified single- and double-stranded DNA by using surface-enhanced Raman spectroscopy on Ag and Au colloids," Chemistry (Easton) 18, 5394-5400 (2012).
2. K. Kneipp, H. Kneipp, V. B. Kartha, R. Manoharan, G. Deinum, I. Itzkan, R. R. Dasari, and M. S. Feld, "Detection and identification of a single DNA base molecule using surface-enhanced Raman scattering (SERS)," Phys. Rev. E 57, R6281 (1998).
3. K. Kneipp, Y. Wang, H. Kneipp, L. T. Perelman, I. Itzkan, R. R. Dasari, and M. S. Feld, "Single molecule detection using surface-enhanced Raman scattering (SERS)," Phys. Rev. Lett. 78, 1667 (1997).
4. E. A. Manrao, I. M. Derrington, A. H. Laszlo, K. W. Langford, M. K. Hopper, N. Gillgren, M. Pavlenok, M. Niederweis, and J. H. Gundlach, "Reading DNA at single-nucleotide resolution with a mutant MspA nanopore and phi29 DNA polymerase," Nat. Biotechnol. 30, 349-353 (2012).
5. T. Ohshiro, Y. Komoto, M. Konno, J. Koseki, A. Asai, H. Ishii, and M. Taniguchi, "Direct Analysis of Incorporation of an Anticancer Drug into DNA at Single-Molecule Resolution," Sci. Rep. 9, 3886 (2019).
6. A. Morita, T. Sumitomo, A. Uesugi, K. Sugano, and Y. Isono, "Dynamic electrical measurement of biomolecule behavior via plasmonically-excited nanogap fabricated by electromigration," Nano Express 2, 010032 (2021).
7. A. Barhoumi, D. Zhang, F. Tam, and N. J. Halas, "Surface-enhanced Raman spectroscopy of DNA," J. Am. Chem. Soc. 130, 5523-5529 (2008).
8. S. Nie and S. R. Emory, "Probing single molecules and single nanoparticles by surface-enhanced Raman scattering," Science 275, 1102-1106 (1997).
9. W. Li, P. H. Camargo, X. Lu, and Y. Xia, "Dimers of silver nanospheres: facile synthesis and their use as hot spots for surface-enhanced Raman scattering," Nano Lett. 9, 485-490 (2008).
10. S. Kogikoski, K. Tapio, R. E. von Zander, P. Saalfrank, and I. Bald, "Raman Enhancement of Nanoparticle Dimers Self-Assembled Using DNA Origami Nanotriangles," Molecules **26**(2021).
11. V. V. Thacker, L. O. Herrmann, D. O. Sigle, T. Zhang, T. Liedl, J. J. Baumberg, and U. F. Keyser, "DNA origami based assembly of gold nanoparticle dimers for surface-enhanced Raman scattering," Nat. Commun. **5**, 3448 (2014).
12. K. Sugano, K. Aiba, K. Ikegami, and Y. Isono, "Single-molecule surface-enhanced Raman spectroscopy of 4,4'-bipyridine on a prefabricated substrate with directionally arrayed gold nanoparticle dimers," Jpn. J. Appl. Phys. 56, 06GK01 (2017).
13. K. Sugano, K. Ikegami, and Y. Isono, "Characterization method for relative Raman enhancement for surface-enhanced Raman spectroscopy using gold nanoparticle dimer array," Jpn. J. Appl. Phys. 56, 06GK03 (2017).
14. C. Chen, Y. Li, S. Kerman, P. Neutens, K. Willems, S. Cornelissen, L. Lagae, T. Stakenborg, and P. Van Dorpe, "High spatial resolution nanoslit SERS for single-molecule nucleobase sensing," Nat. Commun. 9, 1733 (2018).
15. T. Ozaki, K. Sugano, T. Tsuchiya, and O. Tabata, "Versatile method of submicroparticle pattern formation using self-assembly and two-step transfer," J. Microelectromechanical Syst. 16, 746-752 (2007).
16. K. Sugano, T. Ozaki, T. Tsuchiya, and O. Tabata, "Fabrication of gold nanoparticle pattern using combination of self-assembly and two-step transfer," Sens. Mater. 23, 263-275 (2011).
17. C. Munro, W. Smith, M. Garner, J. Clarkson, and P. White, "Characterization of the surface of a citrate-reduced colloid optimized for use as a substrate for surface-enhanced resonance Raman scattering," Langmuir 11, 3712-3720 (1995).
18. K. Sugano, Y. Uchida, O. Ichihashi, H. Yamada, T. Tsuchiya, and O. Tabata, "Mixing speed-controlled gold nanoparticle synthesis with pulsed mixing microfluidic system," Microfluid. Nanofluid. 9, 1165-1174 (2010).
19. M. Giersig and P. Mulvaney, "Preparation of ordered colloid monolayers by electrophoretic deposition," Langmuir 9, 3408-3413 (1993).
20. W. Ke, D. Yu, and J. Wu, "Raman spectroscopic study of the influence on herring sperm DNA of heat treatment and ultraviolet radiation," Spectrochim. Acta A 55, 1081-1090 (1999).
21. X. Yiming, Z. Zhixiang, Y. Hongying, X. Yan, and Z. Zhiyi, "Raman spectroscopic study of microcosmic photodamage of the space structure of DNA sensitized by Yangzhou haematoporphyrin derivative and Photofrin II," J. Photochem. Photobiol. B 52, 30-34 (1999).
22. C. Otto, T. Van den Tweel, F. De Mul, and J. Greve, "Surface-enhanced Raman spectroscopy of DNA bases," J. Raman Spectrosc. 17, 289-298 (1986).
23. E. J. Blackie, E. C. L. Ru, and P. G. Etchegoin, "Single-molecule surface-enhanced Raman spectroscopy of nonresonant molecules," J. Am. Chem. Soc. 131, 14466-14472 (2009).
24. Y. Nishijima, Y. Hashimoto, L. Rosa, J. B. Khurgin, and S. Juodkazis, "Scaling Rules of SERS Intensity," Advanced Optical Materials 2, 382-388 (2014).
25. J. A. Huang, M. Z. Mousavi, Y. Zhao, A. Hubarevich, F. Omeis, G. Giovannini, M. Schutte, D. Garoli, and F. De Angelis, "SERS discrimination of single DNA bases in single oligonucleotides by electro-plasmonic trapping," Nat. Commun. 10, 5321 (2019).
26. K. M. Koo, A. A. I. Sina, L. G. Carrascosa, M. J. A. Shiddiky, and M. Trau, "DNA–bare gold affinity interactions: mechanism and applications in biosensing," Anal. Methods 7, 7042-7054 (2015).
27. K. F. Domke, D. Zhang, and B. Pettinger, "Tip-enhanced Raman spectra of picomole quantities of DNA nucleobases at Au(111)," J. Am. Chem. Soc. 129, 6708-6709 (2007).
28. J. J. Storhoff, R. Elghanian, C. A. Mirkin, and R. L. Letsinger, "Sequence-dependent stability of DNA-modified gold nanoparticles," Langmuir 18, 6666-6670 (2002).